Tunable Mirror and Multi-channel Filter Based on One-dimensional Exponentially Graded Photonic Crystals

Bipin Kumar Singh and Praveen Chandra Pandey
Department of Physics, Indian Institute of Technology (Banaras Hindu University), Varanasi, 221005, India

Keywords: Graded Photonic Crystals, Photonic Band Gap, Omni-directional Band Gap, Exponential Graded Materials.

Abstract: A study on the tunability of photonic and Omni-directional band gaps has been demonstrated theoretically in one-dimensional (1-D) photonic crystals having one of the layers as exponential graded index materials and other layers of constant refractive index materials. Using numerical simulations, we have investigated the effect of relative parameters of exponential graded layers on the photonic and Omni-directional band gaps in 1-D graded photonic crystals (GPCs). We observe that the number of photonic band gaps increases with increase of the layer thicknesses and their bandwidths can be controlled by the contrast between initial and final refractive index of the graded layers. Moreover, we have studied the Omni-directional band gaps in quarter-wave and latent type layer stacking arrangements. Further, we obtained the range of refractive indices and thicknesses of constituted layers at which omnidirectional band gaps occurs. Accordingly, we find that the photonic as well as Omni-directional band gaps of desired bandwidths can be obtained by selecting appropriate parameters in GPCs. Our work will be useful in design of mirrors, channel filters, Optical sensors, Omni-directional reflectors etc. and provide more design freedom for alternative photonic devices.

1 INTRODUCTION

The propagation of light through a periodic medium has been widely researched since the appearance of photonic crystal (PC) materials (Yablonovitch, 1987). PCs are structures composed of two or more materials with different refractive index and arranged in a periodic configuration that forbids the propagation of electromagnetic waves in certain frequency ranges. This leads to a range of frequency where no electromagnetic mode exists within the PCs, is called photonic band gap, which is analogous to the electronic band gap in conventional semiconductors (Joannopoulos, 1997). This property can be used to confine, manipulate and control photons in PCs, and expected to be a key technology for all integrated optical devices (Lipson, 2009). Over the past several years, 1-D PCs have been intensively investigated with different materials such as dielectric, anisotropic, negative refractive index, magneto materials etc. in periodic or non-periodic arrangements (Tolmachev, 2008, Negro, 2005, Alagappan, 2006, Zharov, 2008, Vasconcelos, 2007, Yu, 2007 and Macia, 2012). These have many potential applications in optical communication and optoelectronics such as reflecting mirrors, waveguides, optical switches, filters, detectors, limiters, light emitting diode etc. Moreover, one of the major interesting application of the PCs is the property of Omni-directional reflection by which light with some frequency region from all of the incident angle is totally reflected for both of the TE (Transverse electric) and TM (Transverse magnetic) polarization. The absolute Omni-directional photonic band gap has been demonstrated theoretically and experimentally in 1-D PC structures (Fink, 1998, Yablonovitch, 1998, Seeser, 1999, Xiang, 2010). The Omni-directional band gap has potential applications in reflectors, filters and optical fibers etc.

Recently several other researchers have been proposed the 1-D multilayer structures, in which refractive index or width of layers varies in the form of gradual fashion along the direction perpendicular to the surface of layer (Rauh, 2010, Sang, 2006, Pandey, 2008, Rauh, 2012, Singh, 2013). Such type structures are called graded photonic crystals (GPCs). Gradual variation of relative parameters in GPCs makes them very different in the behaviour from the conventional PCs and enhances the ability to mold and control of the light wave propagation.

Singh B. and Pandey P..
Tunable Mirror and Multi-channel Filter Based on One-dimensional Exponentially Graded Photonic Crystals.
DOI: 10.5220/0005333600220033
In *Proceedings of the 3rd International Conference on Photonics, Optics and Laser Technology* (PHOTOPTICS-2015), pages 22-33
ISBN: 978-989-758-093-2

Graded index materials in one dimensional quasi-periodic photonic crystal have great influence on the optical reflectance and localization modes (Singh, 2014, Singh, 2014).

Motivated by the ability to mold, confine and control of the electromagnetic waves by different types of GPCs. Herein, we study the photonic and Omni-directional band gap characteristics in 1-D GPCs constituted with exponentially graded dielectric layer. Refractive index in exponentially graded layers varies in the form of exponential fashion as a function of the depth of graded layer. This paper is arranged as follows: In Sec. II, the theory and calculation of the reflectance and band structure of 1-D GPC structures is provided. In Sec. III, we investigate the influence of exponentially graded layers on the photonic and Omni-directional band gap properties of 1-D GPC structures. In this Section, our study has been carried out in three steps. First, we present the reflection spectra and band structure of 1-D GPC structures for different layer thicknesses and various refractive index of the constituted normal layer. Second, we investigate the properties of Omni-directional band gap for quarter-wave and latent type layer stacking arrangements. Next, we study the effect of the contrast of initial and final refractive index of the exponential graded layer on the photonic band gap of 1-D GPC structures. Finally, in section IV we have briefly summarized the results.

2 THEORETICAL DESCRIPTION

Here, we present the 1-D GPC multilayer structures as shown in Fig. 1. The GPCs considered in our investigation are composed of two types of dielectric layers. One is the graded layer (A or A′) with exponential varying refractive index as a function of depth of layer and other is homogeneous layer (B) with space independent refractive index. Refractive index profile in the considered exponential graded layers varies in two ways with depth of layer. First, index of refraction increases exponentially from initial to end boundary of the graded layer and is represented as;

$$n(x) = n_i \exp\left(\frac{x}{d_1} \ln \frac{n_f}{n_i}\right) \qquad (1)$$

Second, when refractive index decreases exponentially from initial to final boundary of the graded layer, it can be expressed as;

$$n(x) = n_f \exp\left(\frac{x}{d_1} \ln \frac{n_i}{n_f}\right) \qquad (2)$$

Where n_i and n_f is the lower and higher index of refraction, respectively and d_1 is the layer thickness. In our proposed structures, first case is considered in layer 'A' and second case in layer 'A′'. The two representative structures of 1-D GPCs are a multilayer structure composed with layer A and A′, and their schematic diagram are illustrated in Fig. 1(a) and 1(b), respectively. Refractive index variation in relative proposed structures is also shown in Fig. 1.

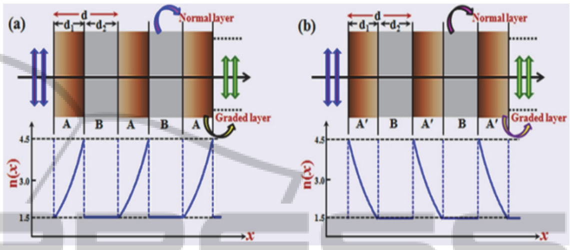

Figure 1: The schematic representation of 1-D graded photonic crystals with exponentially (a) increasing and (b) decreasing refractive index along the thickness of exponential graded layer.

The wave equation for light wave propagation in graded layer, which has exponentially varying refractive index along the plane perpendicular to the surface of layer (suppose *x*-direction) can be written as

$$\xi^2 \frac{d^2}{d\xi^2} E + \xi \frac{d}{d\xi} E + \frac{\xi^2}{\gamma^2} E = 0 \qquad (3)$$

Where, $\xi = \frac{2\pi}{\lambda} n(x)$ is the wave propagation vector for exponential graded layers at normal angle of incidence. Refractive index $n(x)$ taken according the exponential graded layers with increasing and decreasing refractive index defined as above equations (1) and (2), respectively and λ is the wavelength of light. Grading profile parameter for exponentially increasing and decreasing refractive index layers to be $\gamma = \frac{1}{d_1} \ln\left(\frac{n_f}{n_i}\right)$ and $\gamma' = \frac{1}{d_1} \ln\left(\frac{n_i}{n_f}\right)$, respectively. Therefore, we can represent the equation (1) and (2) for the variation of refractive index in the exponential graded layers (A and A′) as $n(x) = n_i e^{\gamma x}$ or $n_f e^{\gamma' x}$ for increasing or decreasing order, respectively. (Yeh, 1988)

The solution of equation (3) can be expressed for increasing refractive index in the exponential graded layers as

$$E(x) = A_G J_0\left(\frac{\xi}{\gamma}\right) + B_G Y_0\left(\frac{\xi}{\gamma}\right) \qquad (4)$$

Where A_G and B_G are arbitrary

constants for graded layers, J_0 and Y_0 are first and second kind of the zero-order Bessel function, respectively. Subscript G represents a graded layer.

Similarly,the solution for exponential graded layers with decreasing refractive index to be similar as equation (4) only propagation wave vector and grading profile parameter changes according to this layer.

The electric field distribution for a homogeneous layer along x-axis can be written as

$$E = A_H \exp(-i\, k_H\, x) + B_H \exp(i\, k_H\, x) \qquad (5)$$

Where, A_H and B_H are the arbitrary constants, k_H is the wave vector and at normal angle of incidence $k_H = \frac{2\pi}{\lambda} n_B$. Subscript H represents a homogeneous layer.

To investigate the propagation properties of the electromagnetic wave in the periodic structures $(AB)^N$ and $(A'B)^N$, where N is the number of periods. We embrace the transfer matrix method to calculate the reflectance and band gap spectra. After applying the transfer matrix approach on the considered structures, if refractive index increases exponentially with depth of graded layers, the electromagnetic wave propagate through the whole structures can be expressed by multiplying the characteristic matrices of the constituent layers as

$$\begin{pmatrix} A_0 \\ B_0 \end{pmatrix} = M_0^{-1}.(M_G.M_H)^N.M_0 \begin{pmatrix} A_{N+1} \\ 0 \end{pmatrix} \qquad (6)$$

Similarly, for the second case if refractive index decreases exponentially with depth of graded layers

$$\begin{pmatrix} A_0 \\ B_0 \end{pmatrix} = M_0^{-1}.(M'_G.M_H)^N.M_0 \begin{pmatrix} A_{N+1} \\ 0 \end{pmatrix} \qquad (7)$$

Where N is the number of the period, A_0, B_0 and A_{N+1} are the arbitrary constant for incident (0^{th}) media and outgoing $(N+1)^{th}$ media, respectively. Matrix M_G and M'_G are the characteristics matrix of exponentially increases and decreases refractive index with depth of graded layers, respectively. Matrix M_H and M_0 is the characteristics matrix of homogeneous layers and air media, respectively.

The reflection and transmittance coefficient of the structures, respectively can be written as

$$R = \left|\frac{B_0}{A_0}\right|^2 \text{and } T = \left|\frac{A_{N+1}}{A_0}\right|^2 \qquad (8)$$

Naturally, due to our consideration of lossless dielectric material, the transmittance here is just the reflectance's complement.

A periodic layer structure is equivalent to a one-dimensional lattice that is invariant under the lattice translation. Here, refractive indices of layers are unchanged by the translation of the wave vector by a lattice constant d, where d is the total thickness of the periodic system. Using the Floquet's theorem, the solution of the wave equation of a period of the electric field for a periodic layer system can be written as $E_K(x,z) = E_K(x)\,.\,e^{-i.\beta.z\, -\, i.K.x}$, where E_K is periodic with period d, i.e. $E_K(x+d) = E_K(x)$ and constant K is known as the Bloch wave number. Hence the dispersion relation for a periodic layer medium can be written as

$$K(\beta,\omega) = \frac{1}{d}\,.\cos^{-1}\left\{\frac{1}{2}(M_{11} + M_{22})\right\} \qquad (9)$$

Where d is the total thickness of a period of the periodic system, M_{11} and M_{22} is the elements of the optical transfer matrix $M_{ij}(i,j = 1{,}2)$. Here, Optical transfer matrix (M_{ij}) of a period equal to $M_G.M_H$ and $M'_G.M_H$ for considered structures with exponentially increasing and decreasing of the refractive index between the boundaries of the exponential graded layer, respectively.

The dispersion relation exhibits multiple spectral bands classified into two regimes: First, where $|(M_{11} + M_{22})/2| \le 1$ corresponds to real K and thus to propagating Bloch waves. Second, spectral bands within which K is complex correspond to evanescent waves that are rapidly attenuated. Defined by the condition $|(M_{11} + M_{22})/2| > 1$, these bands correspond to the stop bands also called photonic band gaps/forbidden gaps since propagating modes do not exist for the systems. [Yeh, 1988].

3 NUMERICAL RESULTS AND DISCUSSION

In this section, we present some numerical results to characterise the optical reflection, band structures, phase shift and Omni-directional band due to the relevant structural parameters of considered 1-D GPC structures. We consider the medium B as homogeneous layer with variable refractive index n_B equal to 1.0, 1.5 and 2.0, while for medium A or A' (Graded layer), we have exponentially varying refractive index with depth of layer in increasing (for layer A) and decreasing (for layer A') fashion between lower refractive index, $n_i = 1.5$ and higher refractive index, $n_f = 4.5$, as expressed by equation (1) and (2), respectively. In this study, we assume that light incident through the air medium and materials are lossless dielectric. Our results observation for the considered 1-D GPC structures constituting exponentially graded index layers has been carried out in three parts.

3.1 Effect of Layer Thickness on Photonic Band Gaps in 1-D GPC Structures

We first present the reflection spectra of 1-D GPC structures at different layer thickness for some selected refractive index of homogeneous layer B under normal incident angle. Thicknesses of the homogeneous and graded layers are chosen as to give, $n_m d_1 = n_B d_2 = D$, where d_1 and d_2 are the thickness of the graded and homogeneous layer, respectively and n_m is the mean value of the initial and final refractive index of the graded layer. For various layer thicknesses, we choose D as $\lambda_0/8$, $\lambda_0/4$, $\lambda_0/2$ and $3\lambda_0/4$, where λ_0 is the optical wavelength and equal to wavelength for the mean value (450 THz) of the considered frequency region (150-750 THz). If layer thicknesses with relative refractive index in structures follow the condition that the layer has an optical thickness one–quarter of the optical wavelength of light, is called quarter-wave layer stacking structures. Similarly, if layer thicknesses with relative refractive index in structures follow the condition that the layer has an optical thickness half of the optical wavelength of light, is known as latent type layer stacking structures. Both type of stacking structures are very useful and suitable for designing various photonic devices. As is evident from the results shown in Fig. 2, there exist a number of photonic bands, where electromagnetic waves cannot be transmitted. The number of photonic bands increases with increasing the thickness of the layers for each chooses refractive index of the homogeneous layer B. Because, with increasing the thickness of layer, the rate of change of refractive index in graded layers increases, and the average refractive index over the volume of each graded layer becomes large. Namely, the rate of change of refractive index contrast of the two types of dielectric layer is enhanced and hence influence the Bragg stack effectively. We also observe that formation reflection spectra are same for the structures with both exponential graded layer A and A′. Fig. 2(a), 2(b) and 2(c), respectively show the reflection spectra of the considered structures for constituted homogeneous layer refractive index, n_B = 2.0, 1.5 and 1.0. For all the chosen refractive index of the homogeneous layer B, formation of photonic bands is similar under normal angle of incidence, but width of bands is different. Bandwidths are larger for $n_B = 1.0$ as compare to other n_B values equal to 1.5 and 2.0. Bandwidths are decreases with increasing n_B values because the photonic band gap properties are basically affected by the contrast of refractive index of constituted media. Contrast of refractive index of homogeneous layer and graded layer is higher for $n_B = 1.0$ as compare to other, therefore the Bragg stack is more effectively and widths of photonic band are large.

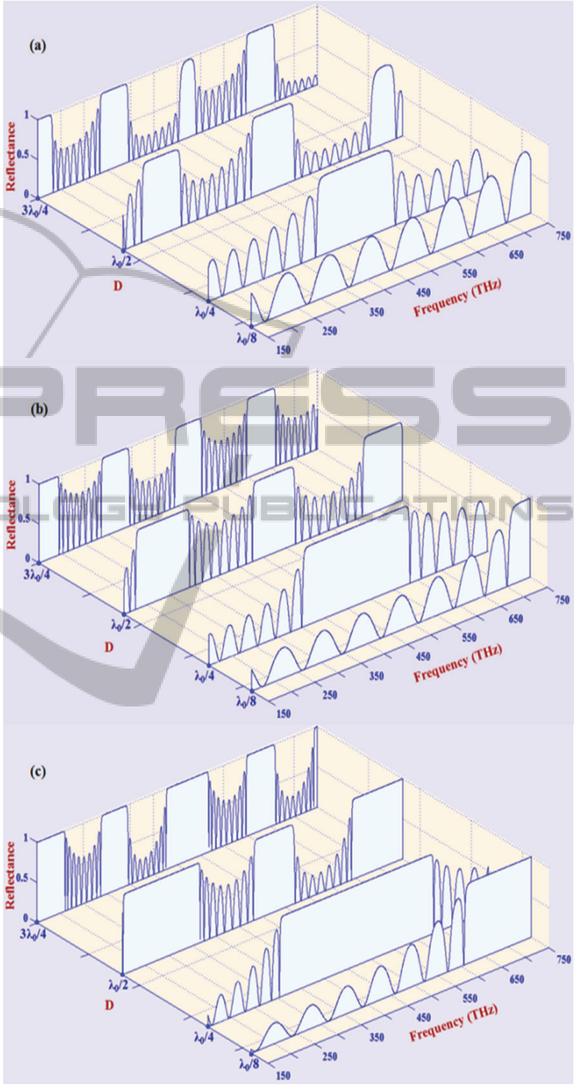

Figure 2: Reflectance spectra of the considered 1-D graded photonic crystal structures for the constituted homogeneous layer refractive index **(a)** n_B = 1.0, **(b)** n_B = 1.5 and **(c)** n_B= 2.0, with various layer thickness constant D.

Now, we examine the confinement effects arising from competition between the structures induced by changing the thickness of layers and magnitude of the total photonic bandwidths in the photonic band gap spectra. To do that, we calculate the regions for forbidden frequencies (stop bands), where $|(M_{11} + M_{22})/2| > 1$, as a function of the thickness of the layers is depicted in Fig. 3(a), 3(b) and 3(c) for the structures with various refractive index of homogeneous layer n_B equal to 1.0, 1.5 and 2.0, respectively. These figures show the distribution of the forbidden (black region) and allowed (white region) frequencies, as a function of the thickness of layers for the structures with n_B equal to 1.0, 1.5 and 2.0 up to the value of D = 9λ$_0$/4. Note that, as expected for large layer thicknesses, we get number of forbidden bands and their bandwidths become narrower and narrower as an indication of more photonic band gaps with small bandwidths. We observe number of forbidden bands are approximate same for the structures with acceptable n_B-values but their bandwidths are different. Total bandwidths in the structures with $n_B = 1.0$ are maximum as compare to other considered n_B-values, which is clearly demonstrated in Fig. 3(d). In this figure, we show the total band gap verses the layer thickness constant (D) for the structures with various refractive index (n_B) of homogeneous layer. It reveals that the total band gaps randomly change with increasing the layer thicknesses, but it is extremun for considered structures with latent type layer stacking arrangements. Therefore, these type structures can be used as mirrors and multi-channel filters by adjusting the layer thicknesses.

For better understanding the effect of graded layer arrangements in the considered 1-D GPCs, we have also calculated the spatial distribution of the square magnitude of the electric field at three selected frequencies impinging under ≈0%, ≈50% and ≈100% reflection conditions for the structures $(AB)^{10}$ and $(A'B)^{10}$, as demonstrated in figure 4. The electric field is denoted by E(x). For the sake of clarity, we have chosen the thickness of layers with relative refractive index equal to 5λ$_0$/4, so the effect of electric field can be better appreciated. From the reflection spectra of the structures with $n_B = 1.0$, it can be clearly observed that at the spectral band edge positions 635THz, where close to 0% reflection is found, reflection is stronger ≈100% within the band gap region than that observed for frequencies 580THz inside the band gap, and at one of the peak at 628.4THz where ≈50% reflection is observed. Therefore, electric field intensity within the considered structures for frequencies 635THz, 628.4THz and 580THz is demonstrated in figure 4(a), 4(b) and 4(c), respectively. Panels (i) and (ii) of the figure 4 show the distribution of electric field intensity in the periodic structures $(AB)^{10}$ and $(A'B)^{10}$, respectively. It is shown that the electric field distributions in exponential graded layers for different grading profiles are quite different,

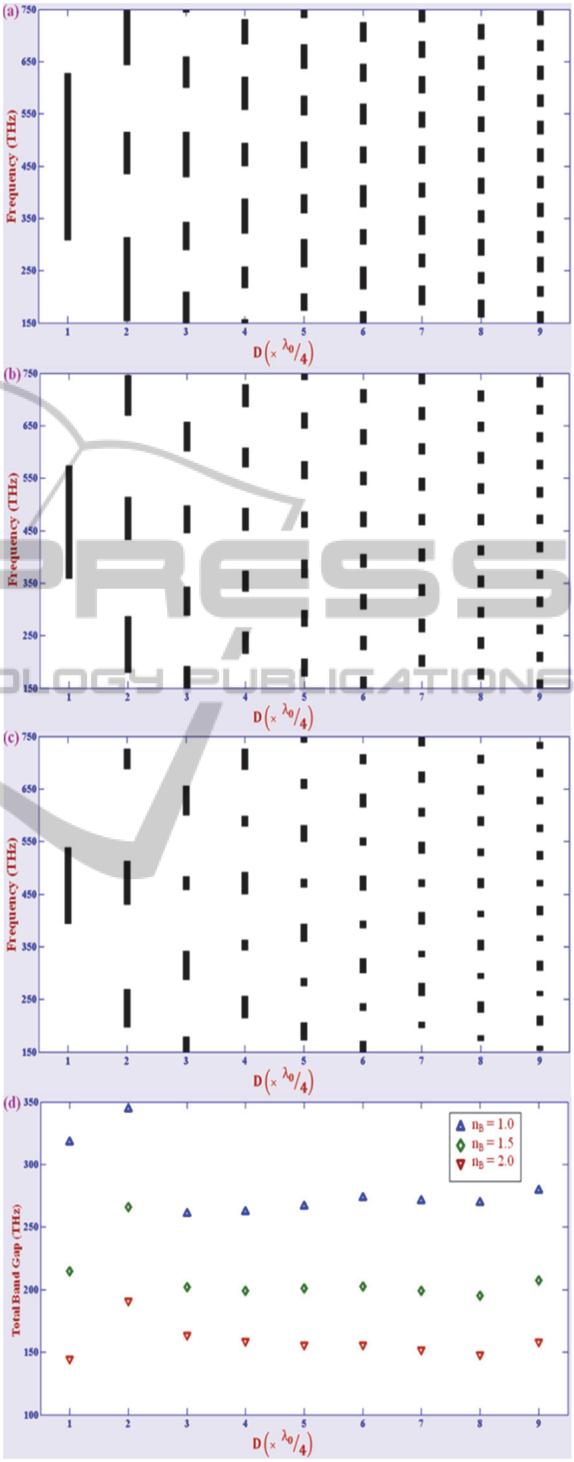

Figure 3: The distribution of the bandwidths as a function of the layer thickness constant D for the structures with homogenous layer refractive index **(a)** n_B = 1.0, **(b)** n_B = 1.5 and **(c)** n_B = 2.0, and plot **(d)** show the total band gap of the forbidden band regions against the layer thickness constant D.

although the volume-average refractive index is same. For exponentially increasing refractive index profile, the electric field intensities in exponential graded layers decrease as propagating depth increases as seen in panels (i), while intensities increase as increases propagating depth for exponential decreasing refractive index as depicted in panels (ii). The reason is the effect of the inhomogeneity in the exponential graded layers. On the other hand, the variation of electric field intensities in graded layers changes due to the space dispersive increasing or decreasing refractive index with graded layers depth. In addition, the electric field intensities in non-graded layers keep unchanged for both types of periodic structures $(AB)^{10}$ and $(A'B)^{10}$.

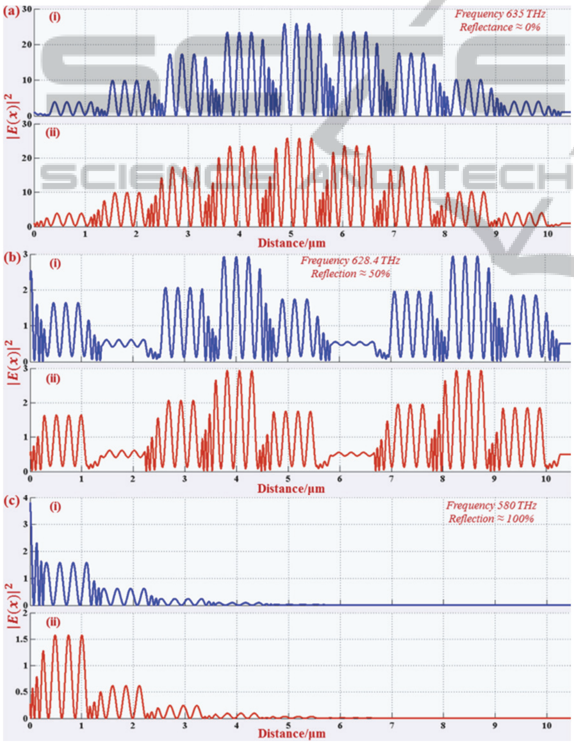

Figure 4: Panels (i) and (ii), respectively show the spatial distributions of the electric field intensity in the systems type1 $(AB)^{10}$ and type2 $(A'B)^{10}$ at three selected frequencies (a) 580 THz, (b) 628.4 THz and (c) 635 THz, impinging under ≈0%, ≈50% and ≈100%, respectively.

Due to the importance of the widespread photonic band gaps for the 1-D GPC structures, we would like to extend the study on the dispersion curves and reflection phase shift associated with the wider photonic band gaps in structures with $n_B = 1.0$. For different layer thicknesses, dispersion curves are calculated from equation (9) for the unbounded periodic structures and shown in panels (i) of Fig. 5 as functions of the reduced Bloch wave vector kd/π, and related reflection phase shifts are likewise illustrated in panels (ii) of the Fig. 5. As expected, the band gaps observed at zero transmission intensity range. The corresponding dispersion curves for the finite crystal are depicted in panels (i) of Fig. 5(a), 5(b) and 5(c), respectively for layer thickness with relative refractive index proportional to $\lambda_0/4$, $\lambda_0/2$ and $3\lambda_0/4$. Also as seen here, number of bands increases with increase in layer thicknesses, single band formed for layer

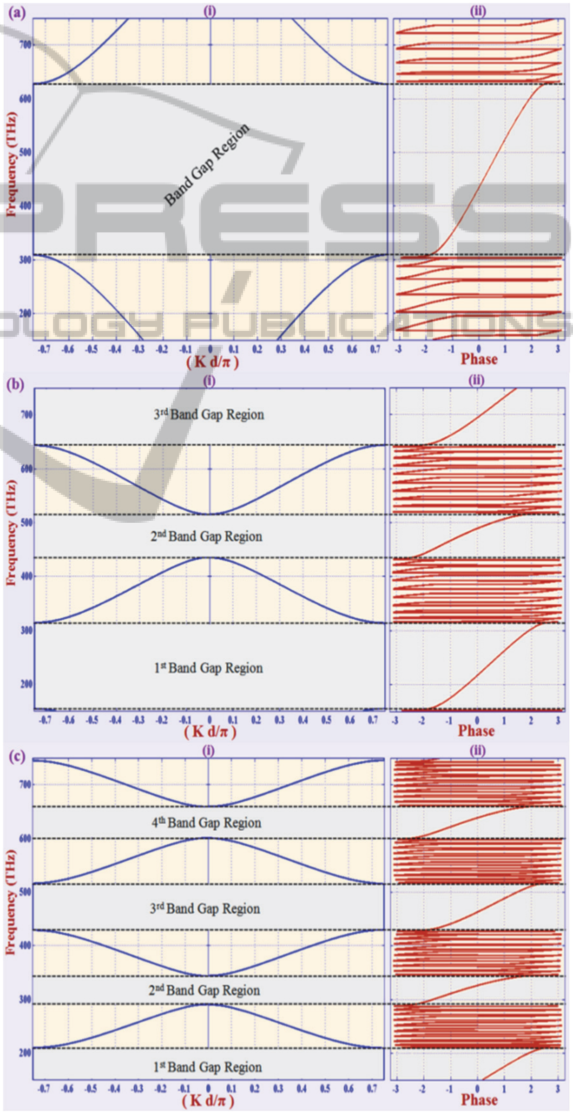

Figure 5: Panels **(i)** and **(ii)**, respectively show the dispersion relationship and phase shifts in a photonic crystal with unit cell consisting of one layer of exponentially graded index material (n_i=1.5 to n_f= 4.5) and other layer of air, for optical layer thicknesses with relative refractive index equal to **(a)** $\lambda_0/4$, **(b)** $\lambda_0/2$ and **(c)** $3\lambda_0/4$**.**

Table 1: Reflection bands region and bandwidths in the GPC structures at normal incidence for different layer thickness.

Layer thickness constant (D)	Structures with n_B = 2.0		Structures with n_B = 1.5		Structures with n_B = 1.0	
	Reflection Band Region	Reflection Band Width	Reflection Band Region	Reflection Band Width	Reflection Band Region	Reflection Band Width
$\lambda_0/8$	……….	……	750.0 – 719.0	31	750.0 – 617.8	132.2
$\lambda_0/4$	538.0 – 393.8	144.2	574.0 – 359.6	214.4	627.0 – 309.0	318
$\lambda_0/2$	269.0 – 197.0	72	287.0 – 179.8	107.2	313.4 – 154.6	158.8
	512.2 – 431.2	81	514.0 – 432.6	81.4	514.8 – 435.4	79.4
	725.8 – 688.4	37.4	746.2 – 669.2	77	750.0 – 643.6	106.4
$3\lambda_0/4$	179.2 – 150.0	29.2	191.2 – 150.0	41.2	209.0 – 150.0	59
	341.8 – 287.6	54.2	342.4 – 289.2	53.2	343.2 – 290.2	53
	483.8 – 459.0	24.8	497.4 – 446.2	51.2	515.6 – 429.2	86.4
	655.8 – 601.0	54.8	656.6 – 601.2	55.4	658.6 – 601.0	57.6
	………………		……………..		750.0 – 745.0	5

thickness with relative refractive index equal to $\lambda_0/4$, three bands for $\lambda_0/2$ and four broader bands for $3\lambda_0/4$, but the bandwidths become narrow with increasing the number of bands. The forbidden bands region and bandwidths of the structures for different layer thicknesses and various refractive index of the homogeneous layer B are listed in Table 1. Moreover, we watch in panels (ii) of Fig. 5 and observe that reflection phase shifts varies from close to $-\pi$ at one band edge to approximate π at another band edge of the stop bands for the precise arrangement of unit cells in structures. Here, we have investigated reflection phase shifts for one of the specified possible arrangements of layers in a period of the considered graded photonic crystal structures.

According to our results, we observe that reflection, transmission and photonic band gap spectra are independent on the arrangement of graded layers (A or A') in unit cells of the structures, whereas field distributions and reflection phase shifts change with arrangement of graded layers in unit cells of the structures.

3.2 Study of the Omni-Directional Band Gap in 1-D GPC Structures

In this section, we discuss the Omni-directional band gap characteristics in the proposed 1-D GPC structures, which have quarter-wave and latent type layer stacking arrangements. An Omni-directional band gap can be obtained within a specific frequency range in photonic crystal as a forbidden band gap that reflects electromagnetic wave at any incident angle for both TE and TM-polarization.

The dependence of photonic band gaps on the incident angle in a quarter-wave stacking multilayer structures for TE and TM polarization are shown in Fig. 6(a & b), 7(a & b) and 8(a & b) for various

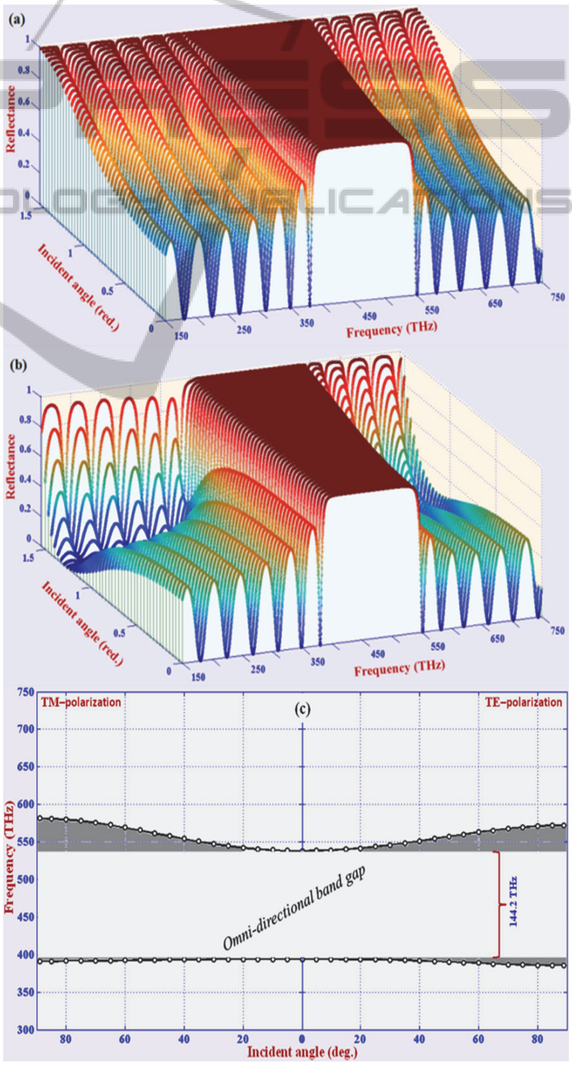

Figure 6: Reflection spectra for **(a)** TE-polarization, **(b)** TM-polarization and **(c)** projected reflection band structure as the changing of the incident angle of the quarter-wave stacking structure with n_B= 2.0.

refractive index; n_B = 2.0, 1.5 and 1.0, respectively. These figures are clearly demonstrated that the expansion of photonic band gap in structures with n_B = 2.0 and 1.5 are enhance for both TE and TM-wave, while for n_B = 1.0, photonic band spreading in frequency range for TE-wave and shrinking in frequency range for TM-wave, when the incident angle increases.

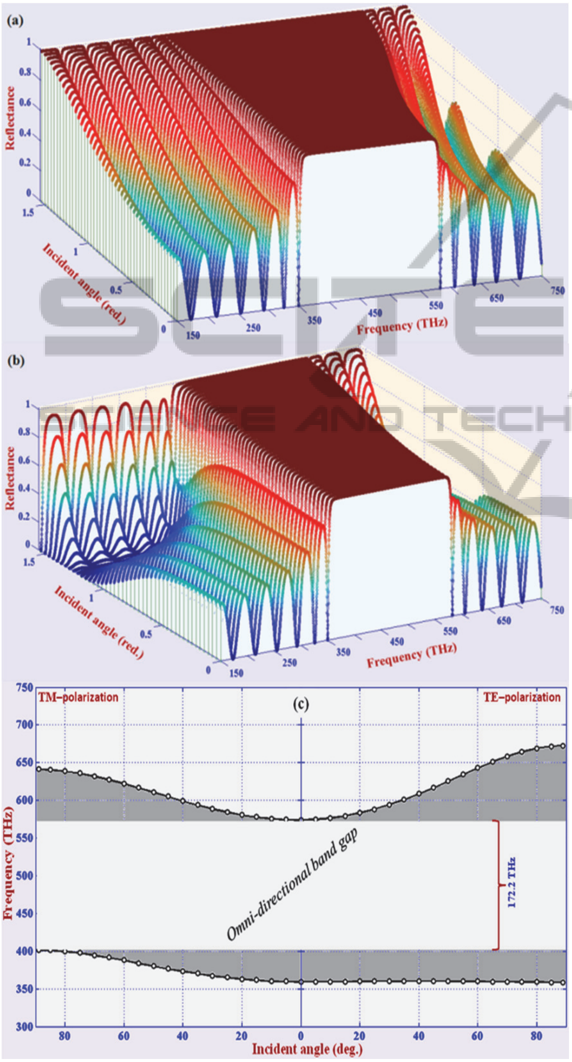

Figure 7: Reflection spectra for **(a)** TE-polarization, **(b)** TM-polarization and **(c)** projected reflection band structure as the changing of the incident angle of the quarter-wave stacking structure with n_B= 1.5.

In order to discuss the Omni-directional band gap properties of the structures, we have plotted the projection band structures as changing of the incident angle and exhibited in Fig. 6(c), 7(c) and 8(c), respectively for the structures with n_B = 2.0, 1.5 and 1.0. From these figures, we can clearly inspect the variation of higher and lower band edges as changing of the incident angle. There is an Omni-directional band gap, which exists between higher and lower band edges as prevalent band region for both TE and TM-polarization. The photonic band spectra of the photonic crystals can be usually achieved from the projection of unit reflectance from Fig. 6(a & b), 7(a & b) and 8(a & b), and Omni-directional band gap clearly demonstrated in Fig. 6(c), 7(c) and 8(c).

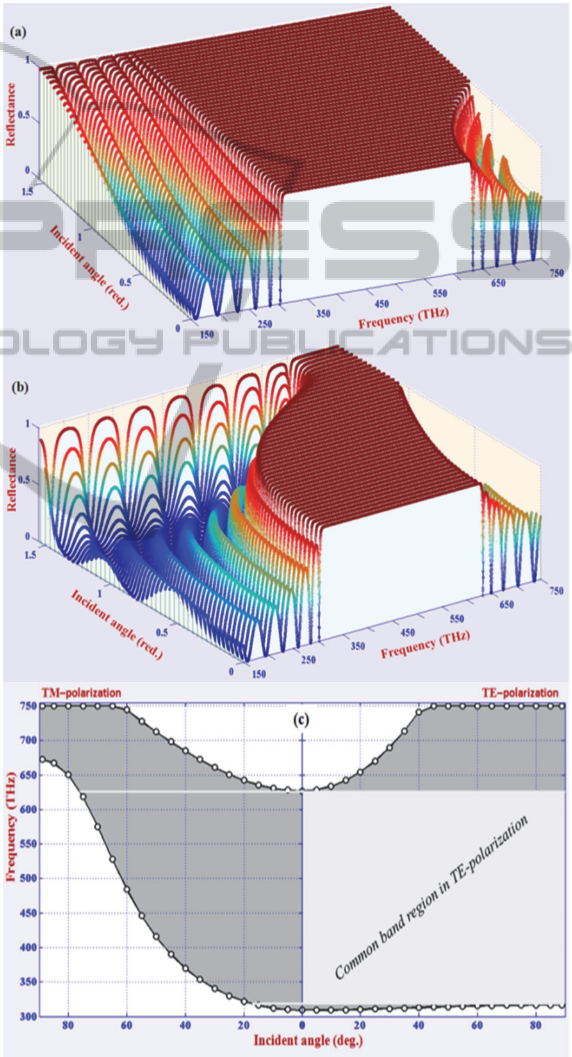

Figure 8: Reflection spectra for **(a)** TE-polarization, **(b)** TM-polarization and **(c)** projected reflection band structure as the changing of the incident angle of the quarter-wave stacking structure with n_B= 1.0.

In Fig. 6(c), 7(c) and 8(c), the grey areas represent the forbidden band for relative polarization and the ubiquitous white area between the band

Table 2: Omni-directional bands region and bandwidths in the GPC structures for various n_B - values.

Structures with	Layer thickness constant (D)	Complete Band Region in		Omni-directional Band Region	Omni-directional Band Width
		TE-Polarization	TM-Polarization		
n_B = 2.0	$\lambda_0/4$	538.0 – 393.8	538.0 – 393.8	538.0 – 393.8	144.2
	$\lambda_0/2$	269.0 – 197.0	269.0 – 197.0	269.0 – 197.0	72
		512.2 – 443.0	512.2 – 464.6	512.2 – 464.6	47.6
		725.8 – 694.0	725.8 – 696.6	725.8 – 696.6	29.2
n_B = 1.5	$\lambda_0/4$	574.0 – 360.2	574.0 – 401.8	574.0 – 401.8	172.2
	$\lambda_0/2$	287.0 –180.2	287.0 –201.0	287.0 –201.0	86
		514.0 – 483.6	514.0 – 502.6	514.0 – 502.6	11.4
		746.2 – 715.6	746.2 – 735.4	746.2 – 735.4	10.8
n_B = 1.0	$\lambda_0/4$	627.0 – 316.8	……….	……….	……….
	$\lambda_0/2$	313.4 – 158.4	……….	……….	……….
		……………..	…………………	……………...	…………………...

edges in both polarizations illustrate the Omni-directional band gap. It is certified from figures, an Omni-directional band exist for structure with n_B = 2.0 and 1.5, while it is not be observed in structure with n_B = 1.0. But one obvious feature of this structure is that there exist broadest complete band gap for TE-wave. Therefore, structure with n_B = 1.0 is more suitable for designing TE-polarized photonic devices and structures with n_B = 2.0 and 1.5 can be used for design Omni-directional photonic devices. Furthermore, we have emphasized the projection band structure as the changing of the incident angle for latent type layer stacking multilayer structures with n_B = 2.0, 1.5 and 1.0. It is clear from our charts, as like a quarter-wave stacking structures, Omni-directional band gap is not exist for structure with n_B = 1.0, but it is obtained for structure with n_B = 2.0 and 1.5. This implies that occurrence of Omni-directional bands is affected by the contrast of refractive index between homogeneous and graded layer, and it is absence for the structures with n_B = 1.0. The number of Omni-directional bands existed for these structures with n_B = 2.0 and 1.5 therefore, these types of structure can be used in the widespread Omni-directional photonic devices which operate in range 150-750 THz. The Omni-directional bands range and bandwidths for the quarter-wave and latent type layer stacking structures with different n_B-values are tabulated in Table 2.

Accordingly, we find that refractive indices of constituted homogeneous layers >1 produce the Omnidirectional band gaps but increasing the indices band gaps become narrowest. Thus the existence of omnidirectional band gaps in graded-homogenous periodicity approach requires the index contrast $(n_m - n_B)$ for n_B>1. But, under this condition, the broader the desired Omnidirectional band range, the greater the demands on index contrast $(n_m - n_B)$, where n_m is the mean value of the initial and final refractive index of the graded layer and n_B is the refractive index of the graded layer. In addition, the omnidirectional band gap can be adjusted by the modifying the layers thicknesses.

3.3 Effect of the Ratio of n_i and n_f on the Photonic Band Gap

Now, we investigate the dependence of the photonic band gap on the ratio of initial and final refractive index i.e. $\left(\frac{n_f}{n_i}\right)$-value of the exponential graded layers in 1-D GPC structures under normal angle of incidence. Here, we considered initial refractive index (n_i) is fixed and equal to 1.5, while, final refractive index (n_f) varies according to contrast value between these. In the Fig. 9(a), we have depicted the refractive spectra for the various $\left(\frac{n_f}{n_i}\right)$-values in a quarter wave stacking multilayer structures with a relatively homogeneous layer refractive index $n_B = 1.0$. As expected, the photonic bandwidth decreases with decreasing the ratio i.e. $\left(\frac{n_f}{n_i}\right)$-values.The explanation for this phenomenon is that decreasing the ratio of initial and final index of refraction of the exponential graded layer, the rate of modification of the grading profile parameter (γ or γ') decreases, and corresponding average refractive index over the volume of each graded layer conjointly decreases, hence influence the Bragg stack become less effectively. However, the photonic band gap decreases with decreasing the grading profile parameter yet obtained band gap exists around the central frequency and it is obviously exhibited in Fig. 9(a).

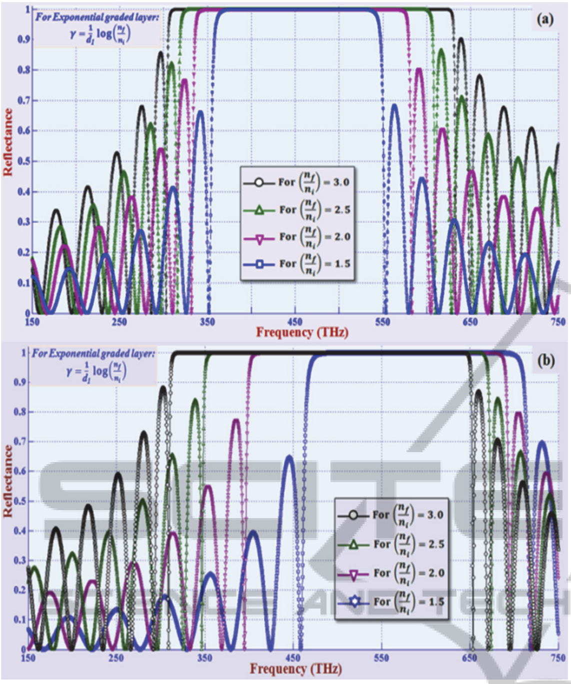

Figure 9: Reflectance spectra for different values of grading profile parameter γ or γ' of exponential graded index layer for the structures with **(a)** quarter wave stacking and **(b)** precise layer thickness d_1 = 64 nm and d_2 = 136 nm.

To have a more complete description and a better understanding of the effect of the ratio of initial and final refractive index of the exponential graded layer on the properties of photonic band gap, it is important to know how these effects change the properties of the reflection coefficients and photonic band gap for the structures with specific layer widths. Here, we also observe that the photonic band gap diminishes with decreasing the grading profile parameter but here acquired band gap is shifted towards the higher frequency region, and it is clearly demonstrated in Fig. 9(b). The explanation for this difference between the above-considered structural arrangements is that, in case of quarter-wave stacking arrangements, the graded layers thickness and grading profile parameter change with the ratio of initial and final refractive index, while in case of the structures with set layer widths, the width parameters are independent of the ratio of initial and final refractive index.

Moreover, we have plotted the forbidden bandwidth by changing the ratio $\left(\frac{n_f}{n_i}\right)$ for a quarter-wave stacking multilayer structure with various relative homogeneous layer refractive indices under normal angle of incidence, which have been illustrated in the Fig. 10(a). In this figure, we see that for a quarter-wave stacking type structures, photonic bandwidth decreases almost linearly. Diminishing of photonic bandwidths is observed for all values of the refractive index ratio greater or equal to the refractive index of the homogeneous layer. But, when the refractive indices ratio of the graded layer becomes lesser than the value of the refractive index of the homogeneous layer than forbidden band width increases gradually and it is clear from third graph for n_B = 2.0 in Fig. 10(a). This reason is the effect of the increase in contrast of the refractive indices of the homogeneous and graded layer. To have a better understanding of the effect of the refractive index ratio on the photonic bandwidths, we have also demonstrated the photonic bandwidths variation by changing the ratio $\left(\frac{n_f}{n_i}\right)$for the structures with different precise layer widths, and it is clearly exhibited in Fig. 10(b). From

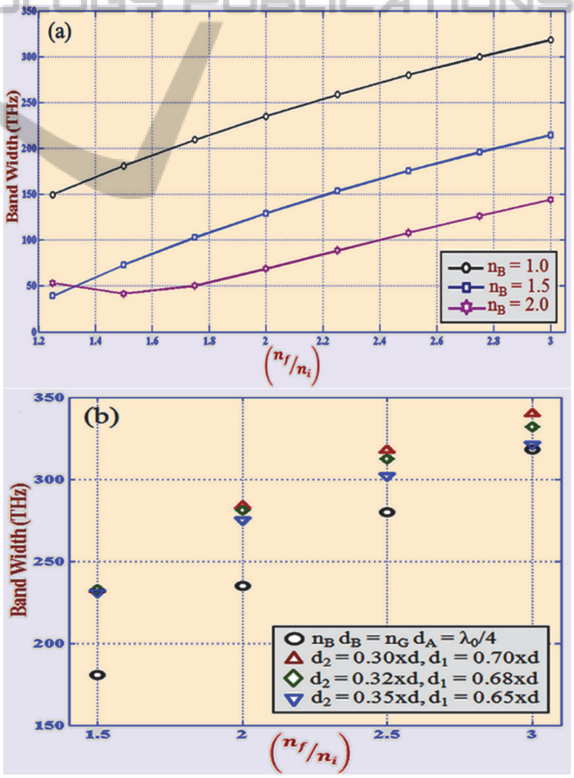

Figure 10: Panel **(a)** shows the distribution of the bandwidths as a function of the ratio (n_f/n_i) for the quarter wave stacking structures with different considered n_B-values and **(b)** exhibits the distribution of the bandwidths as a function of the ratio (n_f/n_i) for the specific layer thickness structures with n_B= 1.0 and d = 200 nm.

Table 3: Reflection bands region and bandwidths in the GPC structures for different (n_f/n_i) values and n_B = 1.0 at normal incidence.

Ratio (n_f/n_i)	Structure with quarter-wave stacking		Structure with constant layers thickness					
			d_1 = 60 nm & d_2 = 140 nm		d_1 = 64 nm & d_2 = 136 nm		d_1 = 70 nm & d_2 = 130 nm	
	Band range	Width	Band Range	Width	Band Range	Width	Band Range	Width
1.5	362.2 – 543.0	180.8	479.6 – 712.4	232.8	472.2 – 705.0	232.8	462.0 – 692.8	230.8
2	340.0 – 575.0	235	412.2 – 695.8	283.6	404.6 – 685.6	281	394.4 – 669.2	274.8
2.5	322.8 – 602.8	280	361.6 – 679.4	317.8	354.2 – 666.6	312.4	344.4 – 646.2	301.8
3	309.0 – 627.0	318	322.4 – 662.6	340.2	315.4 – 647.4	332	305.8 – 626.8	321

this figure, we can watch that for the structures with set layer widths, photonic bandwidth decreases in a parabolic way with diminishing of the refractive index ratio. In these cases, bandwidth also decreases with increasing the exponential graded layer thicknesses. Bandwidths are extremum for lower graded layer thickness and at higher refractive index ratio, but in this figure it is clearly seen that bandwidths are approximately same at lower refractive index ratio for each set graded layer thickness. The photonic bands range and bandwidths for different $\left(\frac{n_f}{n_i}\right)$-values in the quarter-wave stacking and structures with different specific layer widths are tabulated in Table 3.

Accordingly, the average refractive index over the volume of each layer and the different grading profile parameter has great influence on photonic band gaps and their frequency region. Hence, we can tune and achieve the desirable photonic and Omni-directional band gaps by adjusting and tuning the relative parameters of the GPC structures.

4 CONCLUSIONS

In this paper, we have theoretically investigated the tunability of the photonic and Omni-directional band gap characteristics of 1-D GPC structures composed of exponential graded index layers. Here, an exponential graded layer is accomplished by exponential variation of refractive index as a function of layer depth along perpendicular direction to the layer surface. We have observed that the number of photonic bands increases with increasing the layer thicknesses for whatever the refractive index of the constituted homogeneous layer, but their bandwidths decrease with increasing the refractive index of the homogeneous layer. Widths of the photonic bands are also strongly depend on the ratio of initial and final refractive index of the constituted exponential graded layer in 1-D GPC structures, and that are decreasing with diminishing the value of initial and final refractive index ratio. A wide spectral gap is required a high index contrast. Thus, we can control the width of the photonic bands by adjustment of the gradual profile parameters. In addition, we observed that the Omni-directional band exist when we choose the relative refractive index of homogeneous layer equal to 1.5 and 2.0, but it does not exist for 1.0. We found that 1-D GPC structures with relative refractive index of the constituted homogeneous layer equal to 1.5 and 2.0 are appropriate to design the widespread Omni-directional band gap mirrors, filters, reflectors, sensors and other optical devices. For TE-polarization, 1-D GPC structures with refractive index of the homogeneous layer equal to 1.0 has widest common reflection band. Therefore, these structures can be utilized especially for configuration of TE-polarized devices. We realized that the producing of the broader omnidirectional band range demands the high index contrast under the condition of the index of constituted homogeneous layers >1. We expect to achieve desired number of Photonic and Omni-directional band gaps of suitable bandwidths by selecting appropriate parameters in GPCs. Accordingly, our considered structures can be used to design various photonic devices such as mirrors, multi-channel filters and optical sensors etc., which have high ability to control and manipulate light.

ACKNOWLEDGEMENTS

This work has been supported by Department of

Science & Technology DST (INDIA) in the form of project, grant No. 100/IFD2489/2011-12.

REFERENCES

Yablonovitch E., 1987. *Physical Review Letters* 58, 2059 – 2062.

Joannopoulos J. D., 1997. *Nature* 386, 143 – 159.

Lipson R. H. and C. Lu, 2009. European Journal of Physics 30, S33 – S48.

Tolmachev V. A., Perova T. S., Ruttle J. and Khokhlova E. V., 2008. Journal of Applied Physics 104, 033536.

Negro L. D., Yi J. H., Nguyen V., Yi Y., Michel J. and Kimerling L. C., 2005. Applied Physics Letters 86, 261905.

Alagappan G., Sun X. W., Shum P., Yu M. B., Doan M. T., 2006. Journal of Optical Society of America B 23, 159 – 167.

Zharov A. A. and Zharova N. A., 2008. Journal of Applied Physics 103, 013109.

Vasconcelos M. S., Mauriz P. W., de Medeiros F. F., and Albuquerque E. L., 2007. Physical Review B 76, 165117.

Yu Z., Wang Z. and Fan S., 2007. Applied Physics Letters 90, 121133.

Macia E., 2012. Reports on Progress in Physics 75, 036502.

Fink Y., Winn J. N., Fan S., Chen C., Michel J., Joannopoulos J. D., Thomas E. L., 1998. Science 282, 1679.

Yablonovitch E., 1998. Optics Letters 23, 1648.

Seeser J. W., Carniglia C. K., and Dowling J. P., 1999. Science 283, 938.

Xiang Y., Wen S., Dai X., Tang Z., Fan D., 2010. Journal of Applied Physics 108, 093105.

Rauh H., Yampolskaya G. I., Yampolskii S. V., 2010. New Journal of Physics 12, 073033.

Sang Z. F., Li Z. Y., 2006. Optics Communications 259, 174 – 178.

Pandey P. C., Thapa K. B., Ojha S. P., 2008. Optics Communications 281, 1607–1614.

Rauh H., Yampolskaya G. I. and Yampolskii S. V., 2012. Journal of Optics 14, 015101.

Singh B. K., Thapa K. B. and Pandey P. C., 2013. Optics Communications 297, 65 – 73.

Singh B. K., Pandey P. C., 2014. Journal of Modern Optics 61, 887.

Singh B. K., Pandey P. C., 2014. Optics Communications 333, 84.

Yeh P., 1988. "Optical Wave in Layered Media", John Wiley & Sons, Interscience, New Jersey.